Near-source ground motion from steady state dynamic rupture pulses

Eric M. Dunham

Department of Physics, University of California, Santa Barbara, California, USA

Ralph J. Archuleta

Institute for Crustal Studies and Department of Geological Sciences, University of California, Santa Barbara, California, USA

[1] Ground motion from two-dimensional steady state dynamic ruptures is examined for both subshear and supershear rupture velocities. Synthetic seismograms demonstrate that coherent high-frequency information about the source process rapidly attenuates with distance from the fault for subshear ruptures. Such records provide almost no resolution of the spatial extent of the stress breakdown zone. At supershear speeds, S waves radiate away from the fault, preserving the full source spectrum and carrying an exact history of the slip velocity on both the fault-parallel and fault-normal components of motion, whose amplitudes are given by a function of rupture speed that vanishes at $\sqrt{2}$ times the S-wave speed. The energy liberated from the strain field by the passage of a supershear rupture is partitioned into fracture energy dissipated within the fault zone and far-field S-wave radiation. The partition depends on both the rupture velocity and the size of the breakdown zone. **Citation:** Dunham, E. M., and R. J. Archuleta (2005), Near-source ground motion from steady state dynamic rupture pulses, *Geophys. Res. Lett.*, *32*, L03302, doi:10.1029/ 2004GL021793.

1. Introduction

[2] Evidence for ruptures exceeding the S-wave speed continues to mount, most recently in the 2002 M_w 7.9 Denali Fault earthquake [*Ellsworth et al.*, 2004; *Dunham and Archuleta*, 2005]. The ground motion recorded 3 km from the fault at Pump Station 10 exhibited a set of pulses unlike any previously recorded. In light of this record and to further explain features appearing in the model of this event by *Dunham and Archuleta* [2005], we turn our attention to the near-source ground motion of dynamic ruptures. In particular, we discuss how the resolution of dynamic rupture parameters from near-source records depends on rupture speed.

[3] As a starting model, we investigate two-dimensional (2-D) rupture pulses of finite length L, propagating at some steady state velocity V in the positive x direction along the fault plane $y = 0$. We shall refer to the x and y directions as fault parallel (FP) and fault normal (FN). The material on either side of the fault is identical, isotropic, and linear elastic, with shear modulus μ and P- and S-wave speeds c_p and c_s. The steady state assumption implies that we are modeling only the coherent portion of the fields due to a sm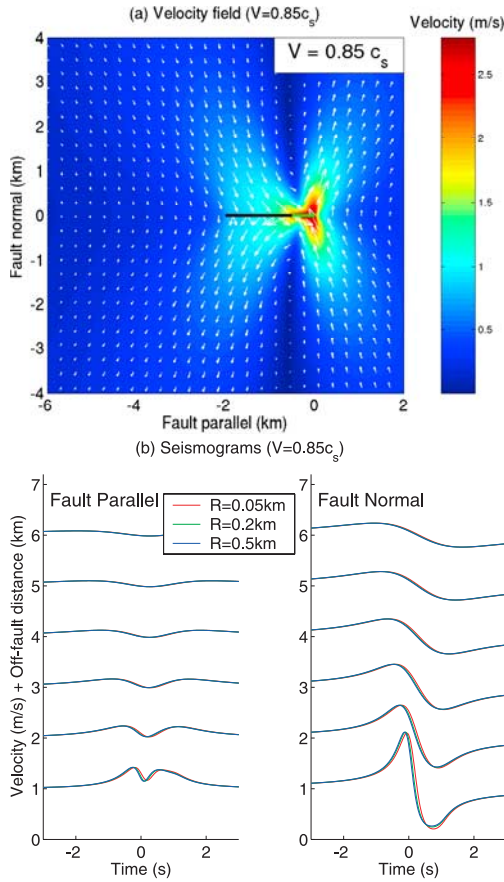ooth rupture process, and not the incoherent high-frequency radiation that results from breaking through small-scale heterogeneities.

[4] We specify the shear traction $\tau(x)$ within the slip zone (unlike kinematic models, which would specify slip). Following *Broberg* [1978, 1989], expressions for the velocity and stress fields, both on and off of the fault, are written in terms of a single integral expression of $\tau(x)$ over the slip zone, weighted by a singular kernel. The expressions are derived in an electronic supplement[1]. *Rice et al.* [2005] have recently evaluated the integral in closed form for the specific case of subshear ruptures in which the shear traction decreases linearly with distance behind the rupture front. In order to accommodate any general $\tau(x)$ and to extend the model to supershear speeds, we numerically evaluate this integral at each observation point, requiring quadrature routines specifically designed to handle integrable and Cauchy-type singularities in the integrand [*Piessens et al.*, 1983].

[5] The elastic fields may be separated into dilatational and shear parts, each governed by the wave equation with the appropriate wave speed. Under steady state conditions, the governing equations become two-dimensional in $x - Vt$ and y. A general field f at speed V may be written as $f(t, x, y) = f^P(x - Vt, y) + f^s(x - Vt, y)$, where f^P and f^s result from a displacement field $\mathbf{u} = \mathbf{u}^P + \mathbf{u}^s$ satisfying $\nabla \times \mathbf{u}^P = 0$ and $\nabla \cdot \mathbf{u}^s = 0$. Using Fourier analysis, we write $f^j(x - Vt, y) = \int_{-\infty}^{\infty} \hat{f}^j(k_x)e^{ik_x(x-Vt)}e^{-k_x\alpha_j y}dk_x$, where $\alpha_j = \sqrt{1 - V^2/c_j^2}$ and $j = p$ or s. This decomposes the response into plane waves $e^{i(k_x x + k_y y - \omega t)}$, subject to the dispersion relation $\omega = c_j\sqrt{k_x^2 + k_y^2}$, and to the condition that the FP phase velocity equals the steady state velocity: $\omega/k_x = V$. For $V < c_s$, both the P and S waves are inhomogeneous. Their amplitude decays exponentially with distance as the observation point moves away from the fault, with the decay length set by the FP wave number k_x and the velocity-dependent factor α_j. When $c_s < V < c_p$, α_s becomes imaginary, and the S waves radiate away from the fault; i.e., $f^s(x - Vt, y) = \int_{-\infty}^{\infty} \hat{f}^s(k_x)e^{ik_x(x+\beta_s y - Vt)}dk_x$, where $\beta_s = \sqrt{V^2/c_s^2 - 1}$. The shear field on the fault is transported without attenuation to observation points off of the fault, enabling a precise determination of the source properties from near-source records of supershear ruptures.

2. Subshear Ruptures

[6] Let us begin with subshear ruptures. We take $t = 0$ such that $x - Vt \rightarrow x$ and place the origin of our coordinate

---

[1]Auxiliary material is available at ftp://ftp.agu.org/apend/gl/ 2004GL021793.

(a) Velocity field (V=0.85c_s)

(b) Seismograms (V=0.85c_s)

Figure 1. (a) Velocity field and (b) synthetic seismograms for a subshear rupture ($V = 0.85c_s$). In Figure 1a the heavy black line denotes the slip zone and the heavy green line the breakdown zone. We take $\tau_p - \tau_r = 20$ MPa, $\mu = 30$ GPa, $L = 2$ km, $c_p = 6$ km/s, $c_p = \sqrt{3}c_s$, and $R = 0.5$ km. In Figure 1b, synthetic seismograms are computed for several values of R as labeled, holding the final slip fixed by varying $\tau_p - \tau_r$. For $R = 0.5$, 0.2, and 0.05 km, the equivalent slip-weakening distances (i.e., the slip at $x = -R$) are $D_c = 0.744$, 0.465, and 0.231 m, the strength drops are $\tau_p - \tau_r = 20.0$, 30.0, and 58.71 MPa, and the fracture energies are $G = 6.66$, 6.23, and 6.03 MJ/m^2. Beyond several km from the fault, the records from all cases are indistinguishable.

system at the leading edge of the slip zone. We use the linear distance-weakening model of *Palmer and Rice* [1973] in which $\tau(x) = \tau_p + (\tau_p - \tau_r)x/R$ for $-R < x < 0$ and $\tau(x) = \tau_r$ for $-L < x < -R$. Figure 1 shows the velocity field and synthetic seismograms. The motion is predominantly in the FN direction, and the synthetics are virtually identical to those from steady state kinematic models [e.g., *Luco and Anderson*, 1983]. As expected on the basis of the Fourier decomposition, increasing the distance between the observer and the fault filters the high frequency components of the wavefield excited by the source process [e.g., *Aki and Richards*, 2002, p.524]. We can estimate the minimum resolvable wavelength for the shear component of the fields $\lambda_{\min}^s$ at some distance y away from the fault in the following manner: Information at a particular frequency becomes irresolvable when its amplitude drops to some fraction,

say 5%, of its amplitude on the fault, leading to the condition $e^{-2\pi\alpha_s y/\lambda_{\min}^s} \sim 0.05$. For $V \sim 0.85c_s$, $\lambda_{\min}^s \sim y$. An even stricter restriction exists for the dilatational fields. This echoes a similar conclusion by *Guatteri and Spudich* [2000], and demonstrates the fundamental difficulty inversions face when using records from subshear ruptures, even without finite bandwidth limitations. On the other hand, our analysis supports the use of kinematic modeling for sub-Rayleigh ruptures, and emphasizes that the parameterization of the slip velocity function will have little effect on the ground motion, so long as the final slip and rise time are preserved.
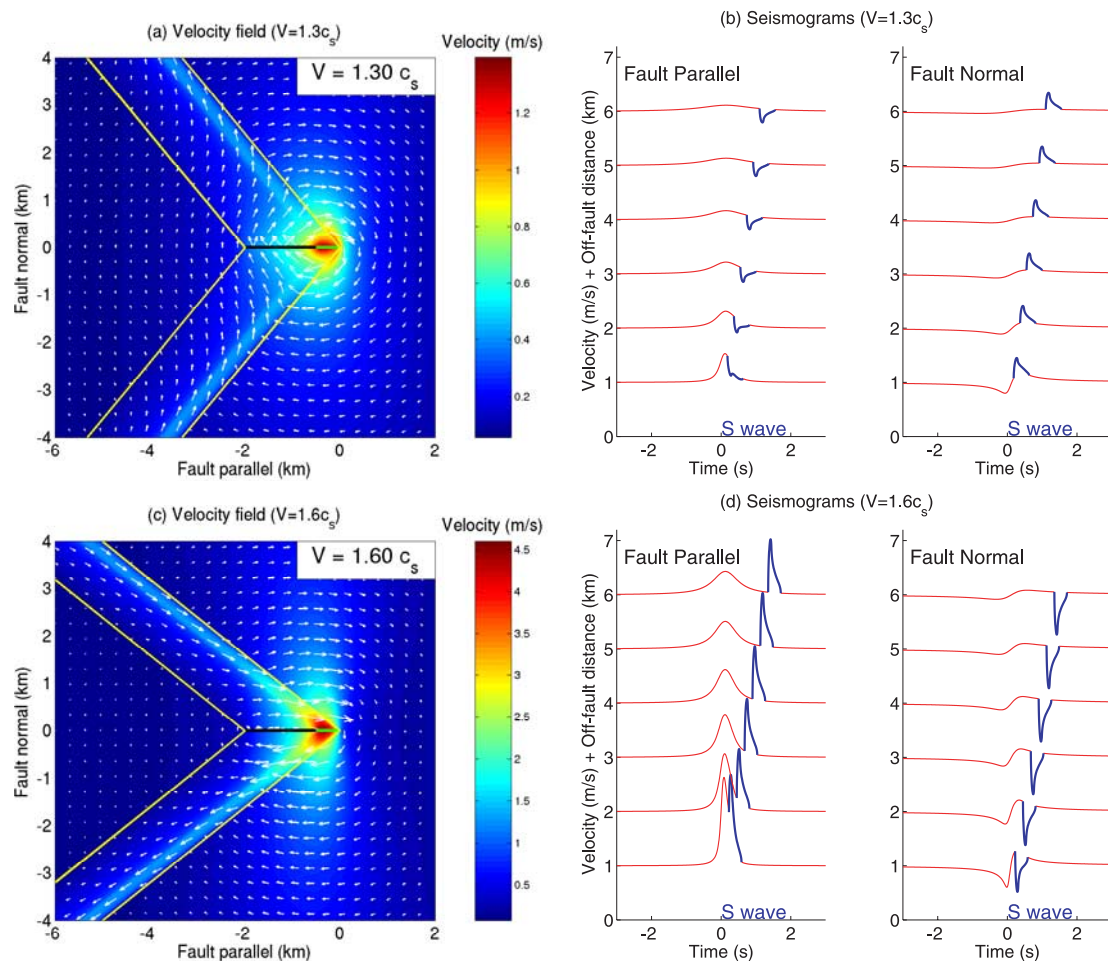
3. Supershear Ruptures

[7] The ground motion from supershear ruptures is shown in Figure 2. Planar wavefronts emanate from the leading and trailing edges of the slip zone. Preceding the arrival of this shear Mach front is the dilatational field, characterized by a circular pattern of rotation around the slip zone. Unless the observer is on the fault, this results in predominantly FP motion, particularly as $V \rightarrow c_p$. In this limit, the P waves become homogeneous and propagate at grazing incidence to the fault with a purely FP particle motion.

[8] The fields change character as V crosses $\sqrt{2}c_s$, the speed at which the S-wave radiation vanishes [*Eshelby*, 1949]. This follows from the expression for the shear traction on the fault in terms of the displacement fields: $\sigma_{xy} = \mu(\partial u_x/\partial y + \partial u_y/\partial x)$, or in the plane wave basis: $\sigma_{xy} = \mu(ik_y u_x + ik_x u_y)$. Choosing a particular V sets both the relative amplitudes of k_x and k_y and the ratio between u_x and u_y since it determines the propagation angle of the radiating wave with respect to the fault. At $V = \sqrt{2}c_s$, a precise balance occurs ($k_x = k_y$ and $u_x = -u_y$), implying that such a wave exerts no shear force on the interface. Conversely, a change in shear traction on the fault (as we model the source process) does not excite S waves. As V crosses $\sqrt{2}c_s$, the relative sign of stress and displacement reverses, resulting in a reversal of the S-wave particle motion.

[9] The ground motion from supershear ruptures contains a wealth of information. The shear field carries an exact history of the slip velocity that appears in both the FP and FN velocity components, as well as in all of the stress components. The velocity fields carried by the S waves are given by $v_x^s(x + \beta_s|y|) = 0.5\,\text{sgn}(y)(\beta_s^2 - 1)/(\beta_s^2 + 1)\Delta v(x + \beta_s|y|)$ and $v_y^s(x + \beta_s|y|) = -(0.5/\beta_s)(\beta_s^2 - 1)/(\beta_s^2 + 1)\Delta v(x + \beta_s|y|)$, where $\Delta v(x)$ is the slip velocity on the fault. The record from even a single station determines both V (from the FP to FN ratio) and Δv.

[10] The direct transport of the slip velocity function off of the fault results in large amplitudes of both velocity and acceleration, particularly if $R/L \ll 1$, as laboratory measurements seem to indicate. As discussed in the previous section, R cannot be reliably estimated from current (sub-Rayleigh) ground motion records. Consequently, the use of large values of R to resolve the breakdown process in numerical models will result in an underprediction of the peak ground velocity and acceleration when the rupture process is supershear.

[11] Pump Station 10 from the Denali Fault earthquake offers the best near-source record of a supershear rupture; however, the station captured waveforms resulting from a

Figure 2. (a, c) Velocity field and (b, d) synthetic seismograms for supershear ruptures having speeds $V = 1.3c_s$ and $1.6c_s$. In Figures 2a and 2c the heavy black line denotes the slip zone and the heavy green line the breakdown zone. The heavy blue lines in the seismograms mark the portions of the records during the passage of the radiated S waves. Parameters are given in the caption of Figure 1.

particularly non-steady rupture process and exhibits motions characteristic of both supershear and subshear ruptures (Figure 3). In the dynamic model by *Dunham and Archuleta* [2005], the rupture accelerates from $0.6c_s$ to $1.5c_s$ approximately 25 km before the station. This process generates a secondary slip pulse moving at the Rayleigh speed. Ground motion pulses A and B (which have a large FP to FN ratio) are generated by the supershear rupture, while pulses C and D (almost entirely on the FN component) arise from the secondary slip pulse. The rapid downward swing in pulse B marks the arrival of the shear field (compare with Figure 2d). Direct extraction of the slip velocity function from the record is not possible for two reasons. The transient emergence of the supershear rupture just prior to the station causes nearly simultaneous arrival of the dilatational and shear field. Furthermore, motions from the secondary slip pulse appear in the tail of the supershear motions. The two-sided FN motions (C and D) are exactly those expected from a subshear slip pulse (Figure 1b), with C being associated with the leading edge of the slip zone and D with the trailing edge. This constrains the width of the slip pulse to approximately 15 km, much larger than appears in the model by *Dunham and Archuleta* [2005],
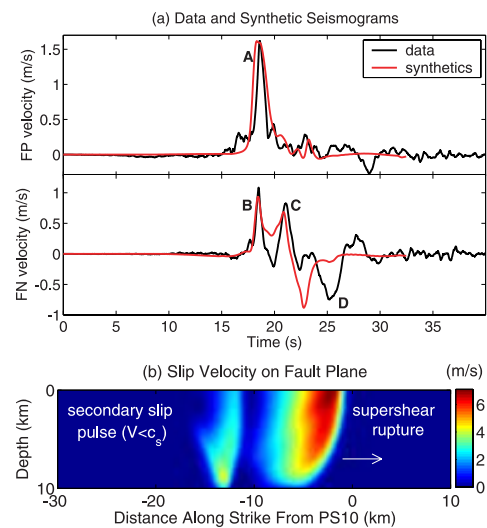
Figure 3. (a) Data and synthetic seismograms at Pump Station 10 (PS10) and (b) a snapshot of the slip velocity on the fault plane for the 2002 Denali Fault earthquake from the dynamic model by *Dunham and Archuleta* [2005].
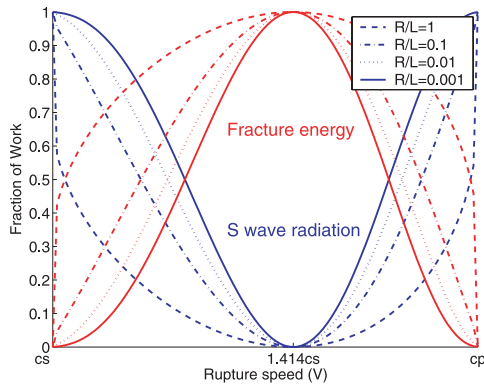
Figure 4. Energy partition between fracture energy and far-field *S*-wave radiation for supershear ruptures as a function of V and R/L for Poisson's ratio $\nu = 1/4$.

who chose parameters to match the narrowness of pulses A and B (at the expense of truncating the width of the secondary slip pulse). The record leaves an open question: What type of rupture process or friction law results in a remarkably narrow supershear rupture pulse but quite broad subshear slip pulse?

4. Energy Balance

[12] The energy balance for dynamic ruptures changes considerably at supershear speeds. For subshear speeds, steady state pulses excite only inhomogeneous waves that do not radiate into the far field. Consequently, all of the strain energy liberated by allowing slip to temporarily relax the stress field dissipates within the fault zone as fracture energy [*Rice et al.*, 2005]. At supershear speeds, the *S* waves radiate and the flux of energy carried by these waves must be taken into account. The proper balance of energy (per unit area advance of the rupture) is $(\tau_0 - \tau_r)\delta = G + G_s$, where τ_0 is the initial (and final) shear traction far in front of (and behind) the slip zone, δ is the final slip, G is the fracture energy, and G_s is the radiated *S*-wave energy (absent for $V < c_s$). The left member of this equation is the work done by the remote stress field in excess of the residual stress, which is the energy available for rupture from the elastic medium. The radiated *S*-wave energy can be calculated by integrating the FN flux of energy over the slip zone: $G_s = 2g_s(V/c_s)\rho \int_{-L}^{0} v_x^2(x, y = 0)dx$, where $g_s(V/c_s) = [(\beta_s^2 - 1)/(\beta_s^2 + 1)]^2/\beta_s$. Dimensional arguments require G

(and G_s) to take the form $h(V/c_s, R/L)(\tau_p - \tau_r)^2 R/\mu$. For subshear ruptures h factors into two terms, the first dependent on V/c_s and the second on R/L. This factorization does not carry over to supershear ruptures [*Broberg*, 1989]. Figure 4 shows the partition of energy as a function of R/L and V/c_s. As R/L decreases, most of the energy is radiated, with the exception of a small range of velocities surrounding $\sqrt{2}c_s$, since no *S* waves are excited at this speed.

References

Aki, K., and P. G. Richards (2002), *Quantitative Seismology*, 2nd ed., 700 pp., Univ. Sci., Sausalito, Calif.

Broberg, K. B. (1978), On transient sliding motion, *Geophys. J. R. Astron. Soc.*, *52*, 397–432.

Broberg, K. B. (1989), The near-tip field at high crack velocities, *Int. J. Fract.*, *39*, 1–13.

Dunham, E. M., and R. J. Archuleta (2005), Evidence for a supershear transient during the 2002 Denali Fault earthquake, *Bull. Seismol. Soc. Am.*, in press.

Ellsworth, W. L., M. Celebi, J. R. Evans, E. G. Jensen, R. Kayen, M. C. Metz, D. J. Nyman, J. W. Roddick, P. Spudich, and C. D. Stephens (2004), Near-field ground motions of the M 7.9 November 3, 2002, Denali Fault, Alaska, earthquake recorded at Pump Station 10, *Earthquake Spectra*, *20*, 597–615, doi:10.1193/1.1778172.

Eshelby, J. D. (1949), Uniformly moving dislocations, *Proc. Phys. Soc. A Gen. Phys.*, *62*, 307–314.

Guatteri, M., and P. Spudich (2000), What can strong-motion data tell us about slip-weakening fault-friction laws, *Bull. Seismol. Soc. Am.*, *90*, 98–116.

Luco, J. E., and J. G. Anderson (1983), Steady state response of an elastic half-space to a moving dislocation of finite width, *Bull. Seismol. Soc. Am.*, *73*, 1–22.

Palmer, A. C., and J. R. Rice (1973), The growth of slip surfaces in the progressive failure of overconsolidated clay, *Proc. R. Soc. London, Ser. A*, *332*, 527–548.

Piessens, R., E. de Doncker-Kapenger, C. W. Ueberhuber, and D. K. Kahaner (1983), *QUADPACK: A Subroutine Package for Automatic Integration*, Ser. Comput. Math., vol. 1, 301 pp., Springer, New York.

Rice, J. R., C. G. Sammis, and R. Parsons (2005), Off-fault secondary failure induced by a dynamic slip-pulse, *Bull. Seismol. Soc. Am.*, in press.

———————————

R. J. Archuleta, Institute for Crustal Studies and Department of Geological Sciences, University of California, Santa Barbara, CA 93106, USA.

E. M. Dunham, Department of Physics, University of California, Santa Barbara, CA 93106, USA. (edunham@physics.ucsb.edu)